Materials & Design 223 (2022) 111233

Contents lists available at ScienceDirect

Materials & Design

journal homepage: www.elsevier.com/locate/matdes

Fabrication of 1D particle structures outside a liquid environment using electric and capillary interactions: From fundamentals to applications

Z. Rozynek [a,b,*], Y. Harkavyi [a], K. Giżyński [c]

[a] Faculty of Physics, Adam Mickiewicz University, Uniwersytetu Poznańskiego 2, 61-614 Poznań, Poland
[b] Department of Battery Technology, Institute for Energy Technology (IFE), Instituttveien 18, NO-2007 Kjeller, Norway
[c] Institute of Physical Chemistry, Polish Academy of Sciences, Kasprzaka 44/52, 01-224 Warsaw, Poland

HIGHLIGHTS

- We demonstrate an uncomplicated and easy to implement method for fabricating 1D microparticle structures outside liquid.
- Different types of microparticles can be assembled in seconds into long chains using an electrical field supported by capillary action.
- Capillary forces were found to help aligning particles and creating one particle–thick structures.
- A comparative study demonstrates that the process functions best in dispersing liquids with high viscosity and low ionic conductivity.
- The 1D structures produced with the new method can be used to create electrically conductive micropaths on a substrate.

GRAPHICAL ABSTRACT

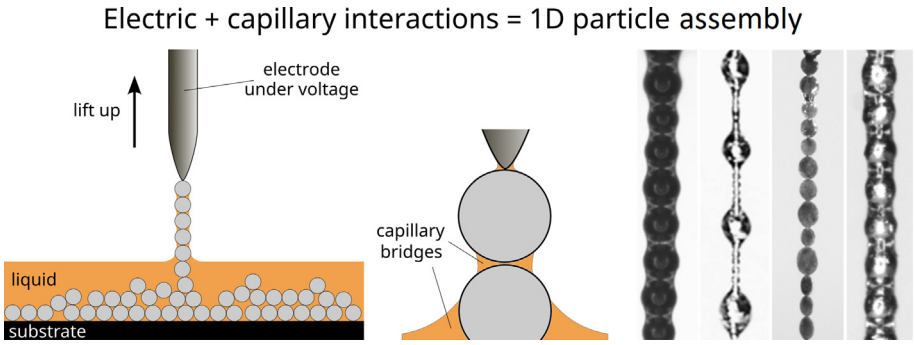

ARTICLE INFO

Article history:
Received 21 April 2022
Revised 3 October 2022
Accepted 4 October 2022
Available online 5 October 2022

Keywords:
1D structures
Particle chain
Beaded structure
Assembly
Capillary bridge
Electric tension
Conductive paths

ABSTRACT

Assembling microparticles into one-dimensional (1D) particle structures formed outside a liquid environment is challenging. This greatly hinders possible applications of such structures and the development of new materials. Herein, we demonstrate a simple, efficient, and easy-to-implement method for fabricating one particle–thick chain-like structures. Electrically conductive particles, initially dispersed in a nonpolar and weakly conductive liquid, are pulled out of the liquid using an electric field supported by capillary action. We study in detail how capillary and electric interactions, viscosity and ionic conductivity of the dispersing phase, particle shape, size and density, and pulling rate affect the general performance of our method. Our experimental results reveal that different types of microparticles can be assembled within seconds to form long chains. We found that capillary forces help aligning particles and creating single particle–resolution structures. The results show that dispersing liquids with large viscosity and low ionic conductivity are preferred as they reduce the negative effect of ionic screening. In the second part of our research, we investigate the physical properties of the produced beaded structures that we deem intriguing for both fundamental and applied research. We finally demonstrate that 1D particle structures can be used to design electrically conductive micropaths.

* Corresponding author at: Faculty of Physics, Adam Mickiewicz University, Uniwersytetu Poznańskiego 2, 61-614 Poznań, Poland.
E-mail address: zbiroz@amu.edu.pl (Z. Rozynek).

https://doi.org/10.1016/j.matdes.2022.111233
0264-1275/

1. Introduction

1D particle structures—their characterization, application, and assembly methods—have been extensively studied over the past few decades. Current research on particle assembly is thriving and largely attracting funding and industry attention worldwide. Low-dimensional particle structures are often considered superior to 2D and 3D assemblies in terms of the added value of the materials after their assembly [1]. The useful properties of 1D particle structures, such as high surface-to-volume ratio, long-range ordering, or periodicity at the mesoscale, can be utilized in a variety of applications, including optical [2–4], biosensing [5], and electronic applications [6–9]. However, the fabrication of 1D particle structures is typically more difficult than the formation of structures with higher dimensionality. There are several approaches for creating 1D particle structures on a substrate. These include magnetic [10,11] or electric field–assisted assembly [12–17], self-assembly on lithographically patterned substrates [18–24], capillary flow–assisted assembly [25,26], self-assembly in pipe-like flows [27], dip coating techniques [28], and acoustic field–controlled patterning [29]. However, it is much more challenging and laborious to create one particle–thick freestanding structures or particle strings formed in air. The limited number of methods available for this type of assembly include transfer printing [30,31], direct writing using liquid metals [32], mechanical manipulation with the use of microrobots, tapered fibers, microneedles connected with hydraulic micromanipulators [33–36], and optical tweezers [37]. These approaches are either expensive, time consuming, or inefficient (*e.g.*, only a limited number of particles can be manipulated in a single step and relatively short particle units can be built when using micromanipulators or optical tweezers). They may also require access to advanced tools and laboratories (*e.g.*, cleanrooms for producing templates or patterned substrates using electron beam lithography or photolithography). This hugely hinders the possible applicability of 1D particle microstructures and development of new materials and devices based on them.

In this study, we demonstrate a simple, efficient, and easy to implement method for fabricating single particle–thick chain-like structures outside a bulk liquid. The experiment can be set up by a nonspecialist in a few hours at a low cost (the budget version of the setup may cost less than a thousand dollars). As briefly communicated in our previous work, the method relies on electric and capillary interactions [38]. The concept of simultaneous usage of electric fields and surface tension is not new. It has been used to guide and concentrate DNA molecules [39], bundled carbon nanotubes [40–44], and silicon [45] or silicon carbide nanowires [46] onto electrode tips to form fibril structures for different applications. In these examples, the electric field was used to dielectrophoretically gather particles at a tip of an electrode, from which the particle structure started to grow, whereas capillary interactions ensured the fibrils had a small diameter. Despite researchers' efforts, a long one particle–thick structure could not be produced in any of the aforementioned works. In this study, we show how this can be achieved. We also provide new essential features of the electric approach for bottom-up assembly (communicated in ref. [38]), which greatly expand the state-of-the-art knowledge in this field. Various aspects of the presented fabricating route, including the role of particle size and shape, physicochemical parameters of the dispersion liquid (*e.g.*, viscosity and ionic conductivity), electric parameters (voltage, frequency), and the role of capillary interactions are here thoroughly studied.

Beaded particle structures have several characteristics that render them unique and useful in many applications. 1D micro and nanostructures that are flexible to a certain extent could find use in crack-free, inorganic coatings, wherein flexible particle wires can form self-assembled coatings that do not crack because of shrinkage in materials for soft robots and responsive matter [47], or in other mechanical applications, such as flexible artificial flagella or cilia [48–50]. Because the physical properties (*e.g.*, mechanical or electrical properties) of the produced beaded structures are intriguing for both fundamental research and applied research, we also design experiments for studying them. In the second part of the work, we present the study results on the macroscopic mechanical properties of freestanding particle chains and electrical properties of 1D particle assemblies deposited on a substrate. The latter can be used as a new type of conductive micropath in electronic applications.

The main outcome of the research is the development and description of uncomplicated and easy-to-implement electric method for fabricating one particle–thick chain-like structures. The results of this research will make the fabrication of 1D materials more efficient and accessible and will unlock the potential of the single particle–thick structures and their unique properties.

2. Methods

2.1. System configurations and experimental setup

The method for fabricating a long 1D particle structure presented here is robust, meaning that it works for various types of particles independently of their size, shape, and electrical properties. It enables formation of 1D structures regardless of the particle density (ρ_p) in relation to that of the surrounding liquid (ρ_l); see Fig. 1a,b.

The experimental setup used for the fabrication of 1D microstructures consisted of a signal generator (SDG1025, Siglent), high-voltage bipolar amplifier (10HVA24-BP1, HVP), digital microscope (AM7115, Dino-Lite), light source (KL 300 LED, Schott), PC for collecting images, and motorized stage (MT1-Z8, Thorlabs) for translating vertically (with a controlled speed) an electrode attached to it through an electrically nonconductive holder. A sample (a thin layer of particle dispersion) was dispensed on a substrate attached to an XY translation stage (LT3, Thorlabs). The stage was used to ease the sample positioning relative to the signal electrode. A schematic figure illustrating the experimental setup is shown Fig. 1c.

2.2. Materials and sample preparation.

Silicone oils (Rhodorsil Oils 47; with different viscosities in the range of 50–1000 cSt at 25 °C, density 0.96–0.97 g·cm^{-3} at 25 °C, electrical conductivity of 5–10 pS·m^{-1}, and relative permittivity ~ 2.8), castor oil (MA-220–1, Mareo, Poland; density of ~ 0.96 g·cm^{-3} at 25 °C, electrical conductivity of ~ 50–100 pS·m^{-1}, relative permittivity ~ 4.7, and kinematic viscosity of ~ 750 cSt at 25 °C), UV-curable epoxy (Formlabs, FLGPCL04; electrical conductivity ~ 100 pS·m^{-1}, relative permittivity ~ 2.7, density ~ 1.1 g·cm^{-3}, and viscosity ~ 2500 cSt, all measured at 25 °C), and liquid flux (TK83, ThermoPasty, Poland; with density 0.85 g·cm^{-3} at 25 °C) were used to form different dispersions with microparticles. We used several types of microparticles: conductive Ag-coated silica microspheres (from Cospheric LCC, USA; M-60-0.17, 55–63 μm; M-60-AG-0.20, 125–150 μm; and M-40-0.67, 10–20 μm, with specific density 0.17, 0.21, and 0.67 g·cm^{-3}, respectively); Ni-plated silica microspheres (from Cospheric LCC, USA; M-18-Ni-0.69, 5–30 μm, with density 0.69 g·cm^{-3}); Cu particles (provided by Prof. Piotr Garstecki from the Polish Academy of Sciences, Warsaw; 40–50 μm, with specific density 8.96 g·cm^{-3});

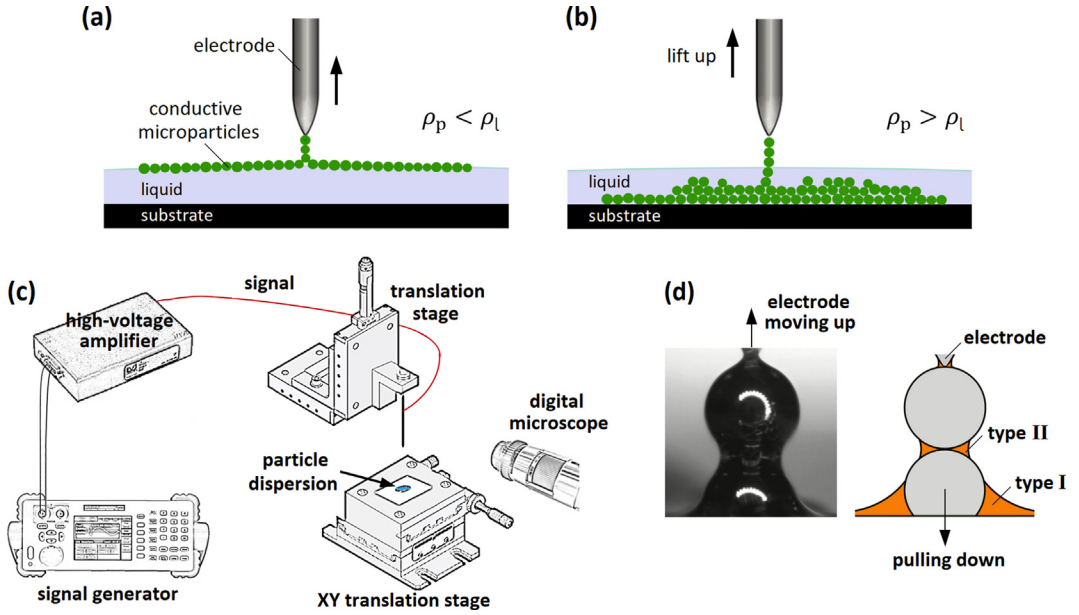

Fig. 1. (a) Lightweight particles float on the surface, and a particle chain is formed at the air–liquid interface. (b) Heavyweight particles sediment at the bottom of the liquid, and a particle chain is formed in the liquid phase. (c) Schematic figure illustrating part of the experimental setup. A high-voltage signal (red line) was provided to the needle-shaped electrode. (d) The image of two conductive particles aligned vertically along the direction of electrode lifting. The lower particle is being pulled out from the liquid. The upper particle is outside the bulk liquid and is in contact with the signal electrode. Two types of capillary liquid bridges are formed, which are well resolved in the image and depicted in the schematic drawing. The force stemming from the particle–planar liquid surface capillary bridge (type I) opposes the electric force by trying to pull the particle down to the bulk liquid (as indicated by the arrow). The particle–particle capillary bridges (type II) aid in stabilizing the chain and influence its mechanical properties. (For interpretation of the references to colour in this figure legend, the reader is referred to the web version of this article.)

solder particles (from IPS, France; $Sn_{96.5}Ag_3Cu_{0.5}$, 45–75 μm); weakly conductive polystyrene particles (from Microbeads AS, Norway; ~140 μm, with specific density of ~ 1.05 g·cm^{-3}, sulfonated for 32 min to increase their electrical conductivity from 10^{-10} to 10^{-7} S·m^{-1} measured at 1 kHz, as described in ref. [50]); stainless steel particles (from Cospheric LCC, USA; 23–28, 41–48, 95–105, and 190–220 μm, with specific density 7.8 g·cm^{-3}). Disc-shaped particles were made by mechanically compressing the solder particles. Hydrogel particles were made of agar powder (~5 wt%, 88588, Sigma-Aldrich) doped with iron nanoparticles (~5 wt%, 637106, Sigma-Aldrich).

3. Results and discussion

3.1. Fabrication of 1D particle structures

A schematic representation of a method for fabricating 1D particle structures is presented in Fig. 1a,b. A signal electrode (here a needle or a thin wire) is first brought close to the interface of a liquid or is dipped into the liquid. An electric voltage (U), applied through the signal electrode, polarizes the particles and attracts them toward the tip of the electrode. As the electrode rises, the particles are successively pulled out from the air–liquid interface on the condition that the strength of the electric force acting on the particle being pulled out from the interface is stronger than that of the force stemming from the capillary bridge (which tries to pull the particle back to the liquid). As the electrode is lifted higher, this particle–planar liquid surface capillary bridge (annotated as type I in Fig. 1d) extends and eventually undergoes a transition into the particle–particle liquid bridge (annotated as type II in Fig. 1d). Meanwhile, a new particle–planar liquid surface capillary bridge is formed at the particle below (see also Movie S1). Once the particle structure of the desired length is formed outside the bulk liquid, the electric tension can be turned off. The newly formed particle chain will remain stable owing to the capillary liquid bridges (type II) that provide attractive interactions between the neighboring particles. In the next section, we will discuss in greater detail the roles of each type of capillary liquid bridges in the 1D particle structure formation, stability, and mechanical properties.

In Fig. 2, we show experimental realizations of the electric route for fabricating 1D particle structures composed of light (floating) and heavy (sedimented) particles. The structures presented in Fig. 2a–e were assembled using a mixture of Ag-coated hollow silica microspheres (with diameter ~ 60 μm) in silicone oil (with viscosity ~ 100 mPa·s). Using a regular mechanical pipette, a few droplets of the mixture were deposited onto the substrate. Because the particle density was much lower than that of the silicone oil, the particles quickly moved upwards, forming a particle layer on the air–silicone oil interface. To initiate the formation of the 1D particle structure, we first lowered the signal electrode to approach the interface (Fig. 2a). Then, we applied an alternating current (AC) electric voltage (U = 500 V, f = 10 kHz, square wave). As a result, the microparticles were attracted to the electrode (Fig. 2b). As the electrode was elevated (with a rate of 0.2 mm·s^{-1}), particles—one after another—were successfully pulled out of the interface forming a structure resembling a beaded necklace (Fig. 2c–e). The particles were held via electrostatic forces and the capillary particle–particle liquid bridges formed by the silicone oil. The whole process is presented in Movie S2.

In the next experiment, we used stainless steel particles (with diameter ~ 100 μm) suspended in the same silicone oil. The suspension was poured into a small glass container. The heavyweight particles sedimented on the bottom of the container. To form 1D particle structures, we used the same electric conditions and similar pulling speeds as those in the first experiment. The particle chain was initiated in a liquid phase (Fig. 2g,h). After lifting the electrode, the particle chain grew as the sedimented particles kept being attracted to the chain's bottom end. Eventually, the structure transited through the air–liquid interface (Fig. 2i) and continued

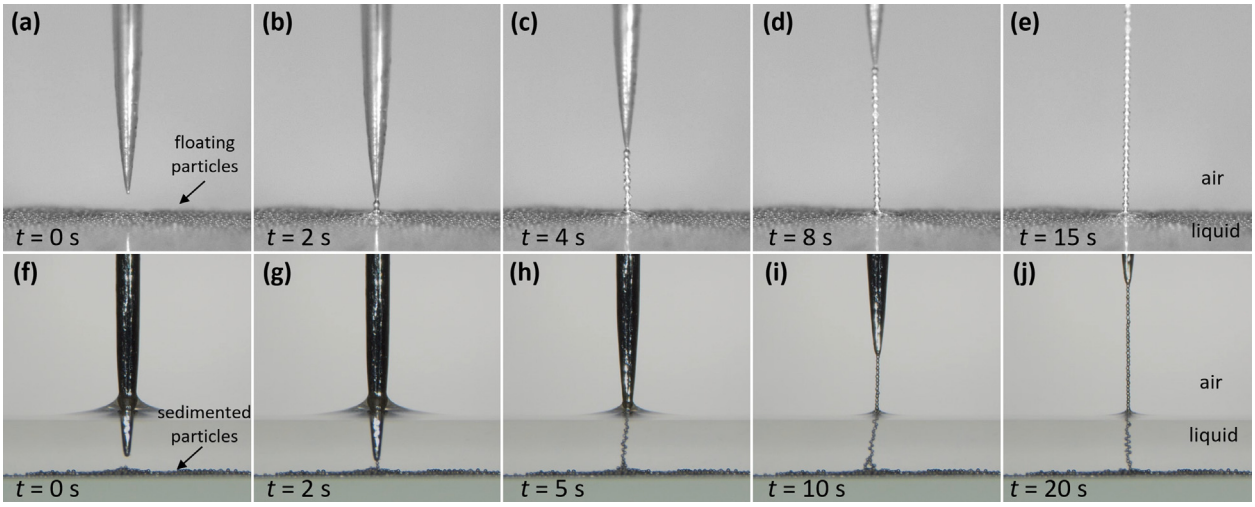

Fig. 2. Fabricating 1D particle structures outside bulk liquid—examples of experimental realization. Images from experiments on (a–e) Ag-coated hollow silica microspheres (size ~ 60 μm), and (f–j) stainless steel particles (size ~ 100 μm) being pulled out of the bulk liquid. In both cases, an AC electric voltage (U = 500 V, f = 10 kHz) was provided to the signal electrode. See also corresponding Movie S2 and Movie S3.

growing to form a 1D particle structure outside the bulk liquid (Fig. 2i,j). See also the corresponding Movie S3.

Fig. 3 summarizes the experimental observations of the 1D particle structure assembly. The electric route presented here enables the formation of long structures comprising hundreds of particles. In Fig. 3a, we show a nearly 3-cm long chain composed of around 600 Ag-coated silica microspheres (size ~ 60 μm) stabilized by silicone oil (viscosity ~ 500 mPa·s). Furthermore, the beaded chains can be made of different particle materials, for example, 100-μm stainless steel particles (Fig. 3b), ~55-μm solder particles (Fig. 3c), and other kinds of electrically conductive materials, such as solid particles of nickel, silver, and gold; or core–shell particles with a conductive shell. Interestingly, these particles can be dispersed in different nonpolar and weakly conductive liquids, such as natural or synthetic oils, liquid paraffin, UV-light curable epoxy (Fig. 3b), or liquid flux (Fig. 3c). We noted that the size polydispersity of particles practically does not affect the structure formation. In fact, we found that the method can be used for creating binary microstructures using a dispersion of two types of particles, *e.g.*, stainless steel particles measuring 45 and 200 μm (Fig. 3d). The particles should be conductive to make a long chain. However, short 1D structures (composed of several particles) can be formed using particles with electrical conductivities several orders of magnitude smaller than those of typical conductors. In Fig. 3e, we present a nearly 2-mm long structure formed outside bulk liquid. It comprises several 140-μm polystyrene particles with electrical conductivity of ~ 10^{-7} S/m (measured at 1 kHz). Apart from solid particles and microspheres, it is also possible to use conductive hydrogel microparticles. In Fig. 3f, we present a chain made of soft spheres composed of agar gel and iron nanoparticles. It is worth mentioning that the method also works for nonspherical particles, such as discs (Fig. 3g) or rods. However, these shapes

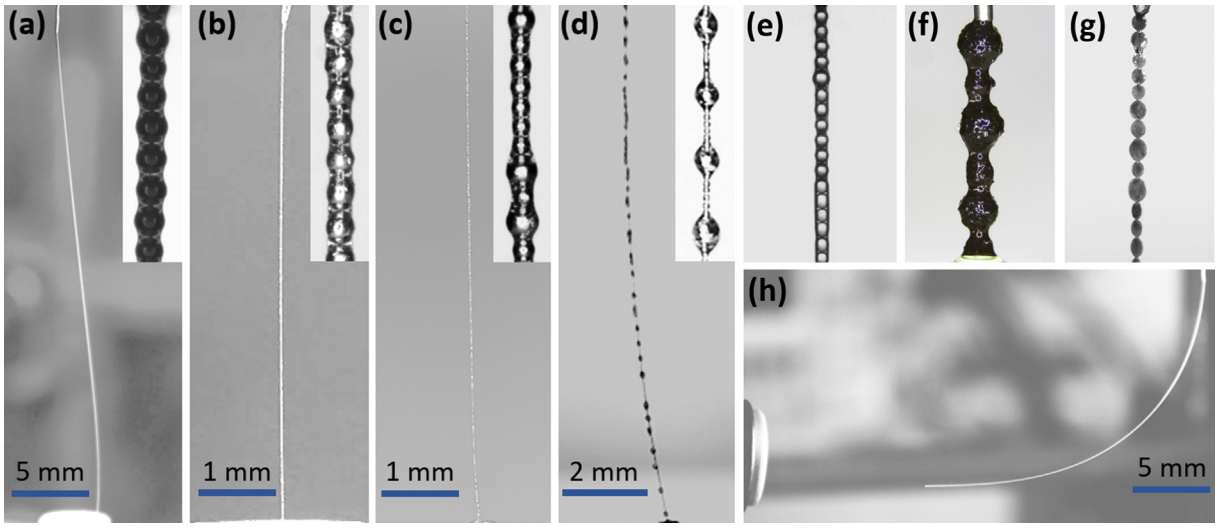

Fig. 3. Viability of the method. The electric method enables the fabrication of single-particle resolution structures made of different types of particles: (a) 60-μm Ag-coated silica, (b) 100-μm stainless steel, (c) $Sn_{96.5}Ag_3Cu_{0.5}$ solder with size 45–75 μm, (d) 45 and 200-μm stainless steel, (e) 140-μm polystyrene with increased electrical conductivity, (f) conductive hydrogel balls with sizes 300–600 μm, and (g) disc-shaped particles with an average diameter of 200 μm. Different liquids were used as dispersing phase, including (a,e,h) silicone oil, (b) UV-curable epoxy, (c) liquid flux, and (d,f,g) castor oil. All the presented structures were stable after turning off the electric tension. The beaded structures were flexible and could bend, as in the example shown in panel (h). See also corresponding Movie S4.

are not favorable because the electric interaction between such nonspherical particles objects is weak and only short structures composed of several particles can be created.

Finally, we observed that all the presented structures were stable after turning off the electric tension, *i.e.*, the particles remained in the chain held by the particle–particle capillary bridges. Interestingly, even small wind drafts in our laboratory did not damage the structures that fluttered and bent, as shown in Movie S4. Their flexibility is also revealed in Fig. 3h, where a long chain (still under the electric tension) bends toward the camera lens seeking the nearest electrical grounding.

3.2. Physics behind the method and its performance

The method relies on the interplay between electric force, gravitational force, and the force stemming from capillary interactions. Additionally, its performance depends on several parameters, such as the electric properties of particles and dispersing liquid, particle wettability, liquid viscosity, particle density, and pulling rate. We will first discuss the role of capillary bridges and the influence of the gravitational force.

3.2.1. Type I capillary bridge

As already noted, there are two types of liquid bridges in the system. The type I capillary bridge emerges upon pulling a particle out from the air–liquid interface, which creates a downward force (F_{sp}) that is the sum of capillary force, buoyancy force, and gravitational terms (hydrostatic pressure and particle weight). The magnitude of this force depends on the shape of the capillary bridge (defined by the particle position (h) in respect to the planar liquid interface; see schematic drawing in Fig. 4a), and its precise estimation is nontrivial and requires numerical calculations (see ref. [51]). Generally, when taking into account a spherical geometry of a particle and assuming that the dispersing liquid is perfectly wetting (justified for nonpolar liquids and various kinds of particles used in this study), the magnitude of F_{sp} scales as $\propto 2\pi R\gamma$ for $R \to 0$ and $\propto R^3$ for $R \to \infty$. Based on our previous theoretical work (ref. [51]), we estimated F_{sp} for two types of particles (light and heavy) with radii (R) between 1 μm and 4 mm, for a given liquid–gas surface tension ($\gamma = 20$ mN·m^{-1}). In Fig. 4a, we plot F_{sp} as a function of particle radius for two different particle densities (0.17 and 7.85 g·cm^{-3}).

From the plot in Fig. 4a, we learn that the gravitational terms are insignificant for a particle with a diameter below ~1 mm. Therefore, the particle density does not play a role for particles in the micrometer scale, *i.e.*, the magnitude of electric force (F_e) needed to pull out a particle (of radius R) from the air–liquid interface is the same independent of the particle density. For a microparticle with a radius ranging between 5 and 500 μm (typically used in this study), the electric force acting on the particle at the air–liquid interface needs to be in a range 10^{-3}–10^{-5}N.

The type I capillary bridge may be deemed an unfavorable physical phenomenon. However, this capillary liquid bridge plays an important role: it aids particle aligning and prevents particle grouping. As shown in Fig. 4b, conductive Ag-coated silica microparticles (sprinkled on a dry substrate) assemble irregularly and form agglomerates when the signal electrode is lifted (see also Fig. S1 and Movie S5). These unwanted features are greatly reduced by the action of the surface tension force. In the bottom panel of Fig. 4b, we demonstrate the formation of a straight, one particle–thick chain, made of the same Ag-coated silica microparticles, pulled out from silicone oil. Note that a chain formed originally with defects can be straightened when pulled through the interface due to the surface tension force (see Movie S6).

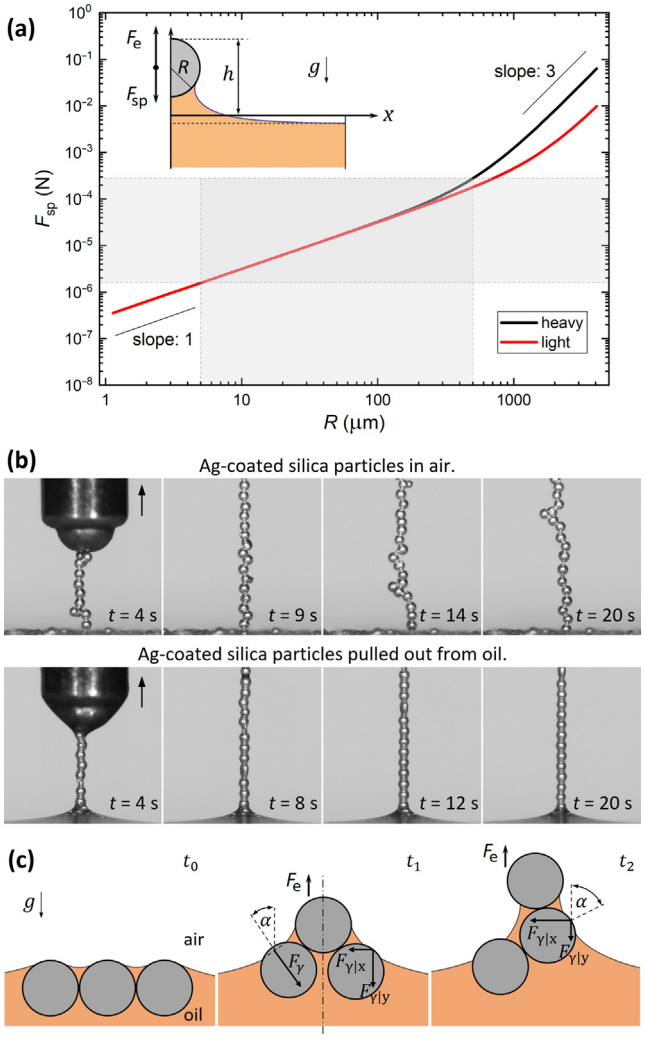

Fig. 4. (a) A log–log plot of F_{sp} as a function of the particle radius R calculated for two different particle densities (0.17 and 7.85 g·cm^{-3}) assuming $\gamma = 20$ mN·m^{-1}. The inset image is a schematic showing the shape of a sphere–planar liquid surface bridge, the direction of force stemming from that bridge (F_{sp}), and the direction of the electric force (F_e). The magnitude of F_{sp} is determined by this shape (assumed as cylindrically symmetric), which largely depends on the relative position h of the particle in respect to the planar–liquid interface. (b) Comparison of chain formation in the air (top row) and pulled out of the liquid (bottom row). Type I capillary bridges are visible at the bottom of the images for the latter case. The electrode was moved upward, as indicated by the arrows. (c) Surface tension helps aligning particles during the formation of a 1D particle structure. At t_0, the particles float at the air–oil interface. Once the middle particle is lifted (by the action of the electric force), the conformation of particles changes and so does the shape of the interface affecting the values of α. This, in turn, influences the magnitude of the components of capillary force, promoting particle alignment in a vertical direction.

As illustrated in Fig. 4c (showing simplified two-dimensional sketch), the capillary force acting on a (second/third) particle can be decomposed into the y component that pushes the particle downward in the direction of gravity $F_{\gamma|y} \sim 2\pi R\gamma \cos\alpha$ and an axial force acting to push the particle sideway just under the above located particle: $F_{\gamma|x} \sim 2\pi R\gamma \sin\alpha$. The angle α comes from the inclination of the air–liquid interface. From the experimental images, we estimated that α changes from nearly 0 to around 75°, indicating that the x component of the capillary force is significant and may indeed play a role in the vertical alignment of particles and the formation of a single particle–thick microstructure. This capillary effect is particularly appreciable for particles with small mass and density for which the gravitational force is too

small to straighten the particle chain (and prevent particle agglomeration).

3.2.2. Type II capillary bridge

When pulling a particle chain out of the liquid, the particle–planar liquid surface capillary bridge (type I) undergoes a transition into the particle–particle liquid bridge (type II).

As described in ref. [51], the capillary bridge transformation can be smooth and continuous or discontinuous (as in Movie S1) depending on the particle diameter. Yet, the character of this transformation does not seem to influence the creation of the 1D particle structure outside the suspension. Remarkably, the presence of the type II capillary bridges makes it possible to reliably hold the formed particle chain even after the electric tension is turned off. This is possible only when the force stemming from the single particle–particle capillary bridge (F_{pp}) is greater than the weight of the chain formed below that bridge. This sets the limit for the maximum number of the particles comprising the particle chain and ultimately defines its maximum length (in the absence of electric force). In Table 1 we present calculations of the maximum number of particles constituting the chain and the chain length for particles with different radii (10–1000 μm) and densities (0.17 and 7.85 g·cm^{-3}). In our calculations, we included the weight of the liquid forming the capillary bridges, assuming the volume of a single bridge is equal to a quarter of the volume of a particle. The liquid density is 1 g·cm^{-3}, and the surface tension $\gamma = 20$ mN·m^{-1}.

From the theoretical calculations, we see that several cm-long 1D particle structures comprising of thousands of particles would remain stable in the absence of the external field. This is, indeed, what we found experimentally. We were able to form a 20-cm long chain made of thousands of Ag-coated hollow silica spheres ($R \sim 30$ μm and $\rho_p = 0.17$ g·cm^{-3}) and a 2-cm chain made of hundreds of steel particles ($R \sim 22$ μm and $\rho_p = 7.85$ g·cm^{-3}).

3.2.3. Pulling rate

As mentioned above, in our calculations we assumed that the volume of a single interparticle bridge is $V_b = V_p/4$. However, the amount of liquid dragged during the particle pulling depends on the pulling speed (v) and liquid's viscosity (η). An example is shown in Fig. 5a, where a chain of particles with a size of ~500 μm is pulled out from a liquid with pulling rates ranging from 0.02 to 1 mm·s^{-1} (gray circles with a yellow rim are added to mark the position of the particles; the black part is the photographed liquid capillary bridge). From an investigation employing particles with radii in the range of 20–500 μm dispersed in silicone oil with viscosities in the range of 10–1000 mPa·s, we find that $V_b \to 0.05\, V_p$ for $(v \cdot \eta)/R < 0.01$ Pa and $V_b > V_p$ for $(v \cdot \eta)/R > 1$ Pa. As presented in Fig. 5b, the magnitude of F_{pp} (stemming from the particle–particle capillary bridge) decreases when V_b increases. Therefore, the maximum length of a freestanding particle chain (attached to the electrode) is determined by the pulling rate.

Moreover, we observe that the liquid bridges stabilize the 1D particle structure when $(v \cdot \eta)/R < 1$ Pa, that is, when $V_b > V_p$. Otherwise, surface tension may cause the particle chain to curl up after removing the electric force (see Fig. 5c). This principle provides a rough estimation of the maximum pulling speed, at which the particle chain can be formed outside the bulk liquid and remains stable in absence of the external force. For instance, for spheres with a radius of $R = 50$ μm dispersed in silicone oil of viscosity $\eta = 50$ mPa·s^{-1}, the maximum pulling speed is approximately 1 mm·s^{-1}; a 1D particle structure with a length of ~1 cm can be formed in just a few seconds. The maximum pulling speed needs to be considered if the electric tension needs to be turned off for any postprocessing work on the assembled structure, unless it is permanently locked (*e.g.*, by hardening of the liquid constituting the capillary bridges) before switching off the electric tension.

3.2.4. Electric effects

As sketched in Fig. 1a,b, the substrate is ungrounded and the direct-current flow is restricted. Thus, the electric circuit can be simplified to the *RC*-circuit, which has two passive components of a resistor (R) and capacitor (C). In such a case, a frequency dependency on the minimal electric voltage (U_{min}) required to pull a particle out from the liquid interface should be expected. We conducted an experiment in which we used Ag-coated hollow silica microspheres (with a density of 0.17 g·cm^{-3}) and investigated U_{min} as a function of its frequency (f). Additionally, we tested the influence of liquid viscosity (ranging from 10 to 1000 mPa·s) on the value of U_{min}. The experimental results shown in Fig. 6a indicate that for high frequencies (f) of the alternating electric field, U_{min} is both viscosity- and frequency-independent, reaching a constant value of around 100 V.

We accept that the following parameters, namely the surface tension (γ), dielectric constants ($\varepsilon_p, \varepsilon_{oil}$), and electrical conductivities (σ_p, σ_{oil}) of the particle and liquid remain constant within the tested frequency range (10–5000 Hz). Such frequency dependence on the electric tension can be understood by a simple analogy to an RC circuit, with the substrate acting as a capacitor. Assume that we apply an AC voltage drop $U(t) = U \cdot \cos(2\pi \cdot f \cdot t)$ to the system. The voltage drops across the capacitor and the resistor, $U_C(t)$ and $U_R(t)$, obey the relations $U_C(t) + U_R(t) = U(t)$, and since $i(t) = R \cdot U_R(t) = C\frac{d}{dt}U_C(t)$, it gives $U_R(t) = RC\frac{d}{dt}U_C(t)$. A Fourier transform yields $\tilde{U}_R(f) = \mathrm{i}2\pi f \cdot RC \cdot \tilde{U}_C(f)$. Given the RC charging frequency $1/f_c = 2\pi RC$, we can derive the voltage drop on a resistor as follows: $\tilde{U}_R(f) = \frac{\mathrm{i}f/f_c}{1+\mathrm{i}f/f_c}U$. To pull a 1D particle structure out of the silicone oil, we need a sufficiently large electric force between spheres, which is determined by the magnitude of the voltage drop $\left|\tilde{U}_R(f)\right|$. Considering $\tilde{U}_R(f) = U/\sqrt{1+(f_c/f)^2}$, the threshold in the total applied electric tension U should then be: $U_{min} \propto \sqrt{1+(f_c/f)^2}$. This is consistent with the experimental observation, that is, at high frequency, the threshold voltage U is independent of the field frequency; however, at a low frequency, U_{min} is nearly inversely linear with f.

3.2.5. Dispersing liquid viscosity and its ionic conductivity

The results in Fig. 6a also show that for each oil viscosity value, there is a different threshold frequency (f_{th}), below which the value of U_{min} increases. We collapsed the data presented in Fig. 6a by multiplying each curve by its corresponding viscosity value (see Fig. 6b). The data collapsed reasonably well, indicating

Table 1
Calculated maximum number of particles making up the chain and the chain's length for particles of different radii (R) and densities (ρ_p).

R[μm]	10	20	50	100	200	500	1000
no. particles ($\rho_p = 7.85$ g·cm^{-3})	~4×10^3	~1×10^3	~150	~40	~10	~1	0
length$_{max}$ [cm]	~4	~2	~0.75	~0.4	~0.2	~0.05	–
no. particles ($\rho_p = 0.17$ g·cm^{-3})	~7×10^4	~2×10^4	~3×10^3	~700	~200	~30	7
length$_{max}$ [cm]	~70	~40	~15	~7	~4	~1.5	0.7

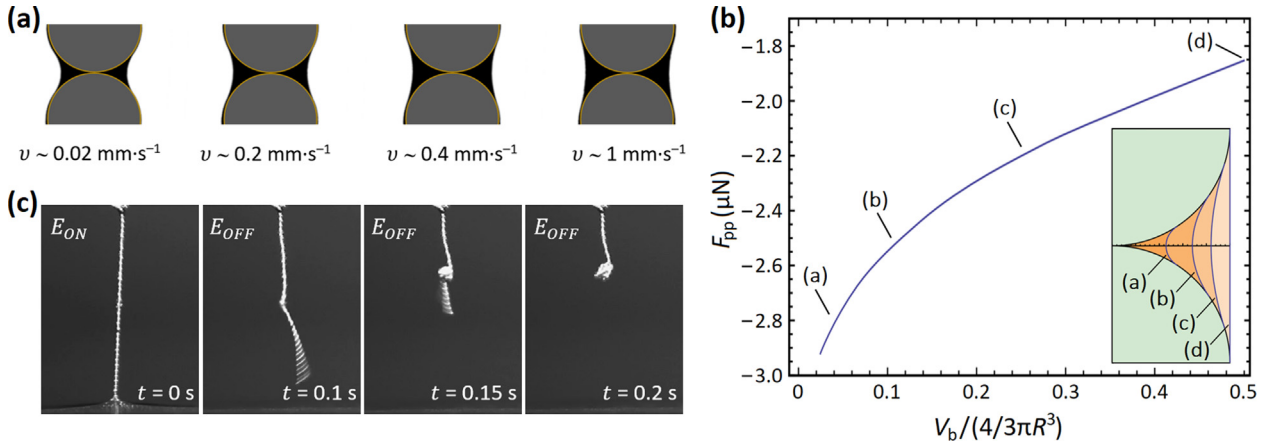

Fig. 5. (a) Stainless steel particles (size of ~500 μm) pulled out from silicone oil (~100 cSt) with different pulling rates 0.02–1 mm·s^{-1}. The amount of liquid dragged during the particle pulling depends on the pulling speed (and the liquid's viscosity). (b) The magnitude of the force F_{pp} plotted against the dimensionless volume of the particle–particle capillary liquid bridge. The calculations were performed for particles with $R = 25$ μm and $\gamma = 20$ mN·m^{-1}. Note that the plot starts from $V_b/V_p = 0.02$, as the lower values would not be physical, *i.e.*, for the given surface tension and the atmospheric pressure, it is not possible to form a bridge with $V_b/V_p < 0.02$ even if the pulling rate would go to zero. The inset image shows schematically-four examples of different shapes of the capillary liquid bridge with their corresponding dimensionless volumes V_b/V_p. (c) A particle chain made of Ag-coated silica microspheres (~60 μm) pulled out from silicone oil at 1 mm·s^{-1}. Due to the surface tension of the liquid (with $V_b > V_p$), the chain curls up after the electric tension is turned off.

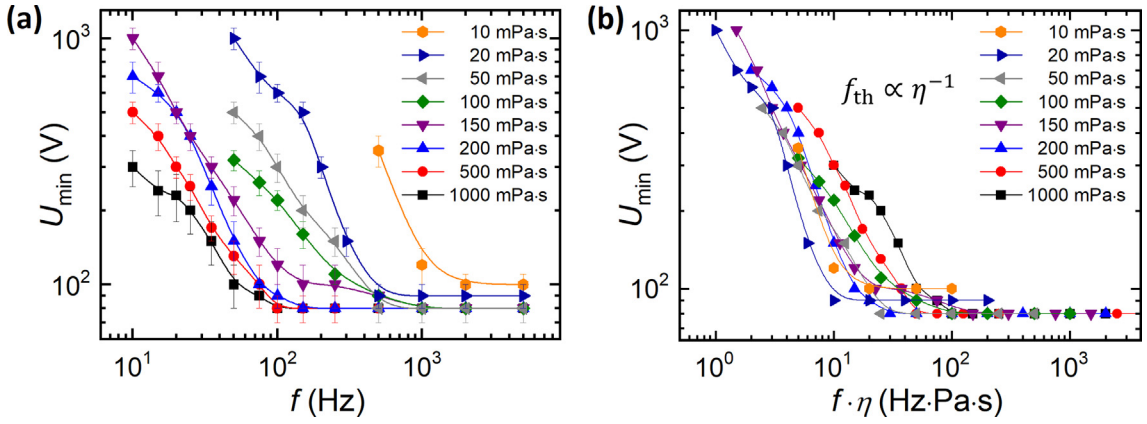

Fig. 6. Minimum electric tension required for pulling a particle out from the interface. (a) Below a threshold frequency, U_{min} is f-dependent, whereas at high frequencies, U_{min} reaches a constant value of around 100 V. (b) The collapsed data reveal scaling of the threshold frequency (*i.e.*, $f_{th} \propto \eta^{-1}$).

that $f_{th} \propto \eta^{-1}$ (see also Fig. S2, where we plot f_{th} vs η). This transition frequency f_c can be associated with the electrostatic screening of the electric field by ions (impurities) present in the oils. For the oils in the viscosity range studied here (*i.e.*, 10–1000 mPa·s), the ionic diffusivity is inversely proportional to viscosity [52]. This may explain the shift of the threshold frequency toward higher frequency values for the oils with smaller viscosities featuring greater ionic diffusivity.

Furthermore, to investigate the influence of ions, we conducted an experiment using both pure and modified silicone oils (with viscosity $\eta = 350$ mPa·s). The latter possesses an increased concentration of mobile ions, increasing the ionic conductivity, provided from a dissolved quaternary ammonium salt. As shown in Fig. S3, the addition of ions affects the $U_{min}(f)$ curve by shifting it toward higher frequency values, which is consistent with the abovementioned results.

Generally, we observed that the proposed electric method for fabricating 1D particle structures outside the bulk liquid works better for dispersing liquids with viscosities much larger than that of water and with ionic conductivity lower than around 10^{-9} S·m^{-1}. Otherwise, a frequency greater than 10 kHz must be used to suppress the unfavorable effect of electrostatic screening. Increasing the magnitude of electric tension may also help by generating stronger electric force between particles. However, it leads to increased electric current flowing through the particle chain, which could be ultimately destructive. We noted that the heat generated by the high current flow caused the degradation of the fluid and/or damaged the hollow particles with thin shells, thus preventing the formation of a long and stable particle chain.

3.3. Toward applications

The assembly method we describe here is simple, efficient, and easy to implement. As mentioned in the Introduction, the experimental setup can be assembled within hours and is inexpensive (starting from around $1000). The formation of 1D particle structures can be parallelized if needed, enabling simultaneous assembly of dozens of chains. As demonstrated in the previous section (see Fig. 3), the particle structures can be designed to be several centimeters long and composed of thousands of particles. Such a low-cost and relatively efficient method should find use in different applications. Therefore, our method could lead to new approaches of organizing particles that could be utilized in both fundamental studies and applied research. In this section, we

demonstrate two application examples of the method. We will begin with presenting the formation of particle chains for studying their intrinsic mechanical and electric properties.

3.3.1. Fabricating particle chains to study their mechanical properties

There are several research studies on the mechanical properties of locked/fused granular and colloidal chains in the absence of external fields, where researchers investigated their elasticity, flexibility, or stretchability [16,53]. These mechanical properties are often attributed to the intrinsic properties of the locking material, such as grafted DNA [54,55] or polymer crosslinkers [56], that forms flexible joints connecting rigid micro or nanoparticles. Unfortunately, very little is known about the mechanical properties of capillary bridges–joint particle assemblies forming 1D particle structures. In particular, the literature lacks studies on the mechanical properties of such systems produced outside a bulk liquid and subjected to electric tension. The reason for this could be the difficulty in producing such single particle–resolution structures.

Here, we present the preliminary results of our ongoing project, in which we investigate the mechanics of a freestanding particle structure and study in detail the role of particle size, liquid viscosity, and dielectric properties, as well as the magnitude of the electric tension on the mechanical parameters of a particle chain. In the first example, we fabricated a short (~3 mm) particle chain made of stainless steel particles (~100 μm). One of its ends was attached to a pointy piece of a nonconductive substrate. The substrate was placed on a mechanical stage that moved vertically. By moving the substrate up and down we could change the mechanical compressive force acting on the chain. We varied the strength of the electric tension (100–450 V) applied to the electrode and studied qualitatively how the compressive mechanical stress is absorbed by the particle chain. As presented in Fig. 7a–e, the bending stiffness increases as the electric tension increases. It is interesting to see that at low electric tensions, the mechanical stress absorption is through particle structure buckling (see panels a,b). In contrast, at high electric tensions, the particle chain bends (see panels d,e).

To gain a deeper insight into the particle chain stability, we performed additional experiments on its mechanical properties. We formed a chain that spanned between a static electrode and an electrode that could rapidly translate in the vertical direction, normal to the gravity direction (see Fig. 7f). By moving the electrode by ~ 0.25 mm (the initial position of the electrode is indicated by the shaded image in the top panel of Fig. 7f), we created a downward motion to form a transverse wave propagating along the particle chain. The propagation velocity of the wave was recorded using a high-speed camera replacing the digital microscope (shown in Fig. 1c). We extracted four images (see Fig. 7f) from the movies to estimate the magnitudes of wave propagation velocities. We repeated the experiment for different magnitudes of electric voltage (between around 20 and 400 V) and estimated the wave propagation velocity. The results are plotted in the Fig. 7g. The velocity of the wave propagation v, the tension $F_T \propto v^2$ along the particle chain, and the bending stiffness $K \propto F_T$, all sharply increase with the magnitude of the electric tension above 100 V, making the 1D particle structure less flexible. The experimental data points were fitted to the formula $v = C_1 + C_2 \cdot U^2$, where the first term is the contribution from the capillary interactions and the second term describes the electric relationship. The fitting curve captures the trend relatively well, although more quantitative data is needed to be conclusive on the role of the electric tension on the mechanics of the particle chain. Nevertheless, we demonstrated that the electric method can easily produce a particle chain outside the bulk liquid and that the chain's mechanical properties could be studied to enhance the fundamental knowledge.

3.3.2. Formation of conductive micropaths and studies of their electric properties

Regarding the electronic properties of 1D particle microstructures, if the neighboring particles in the 1D particle structures are physically connected and the electrical resistivity is kept as low as in the bulk particle material, it should make them excellent candidates for conductive paths that are far cheaper than the

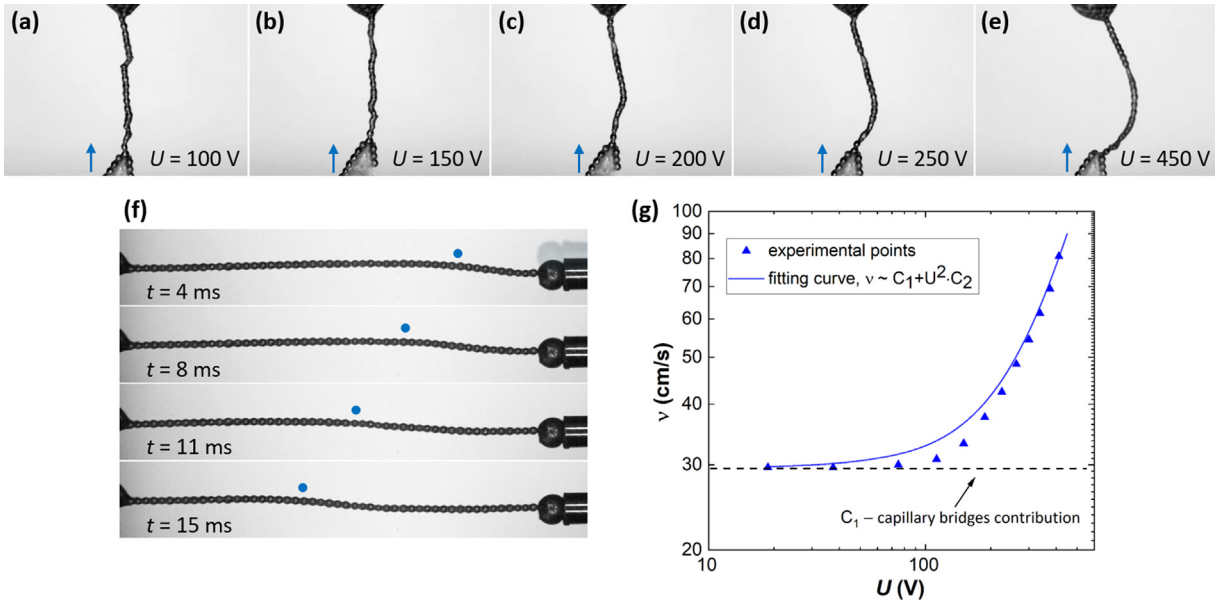

Fig. 7. Mechanical properties of a particle chain under electric tension. (a–e) Buckling to bending transition of the 1D particle structures under mechanical compression observed at increased electric tension. A pointy piece of a nonconductive substrate (to which a bottom end of the chain was attached) was moved up and down to change the mechanical compressive force acting on the chain. (f) Images of a particle chain made of stainless steel particles (~100 μm) captured at different times show the propagation of a transverse wave. The front of the wave is marked with a dot. (g) The velocity of wave propagation (v) plotted against the applied electric tension (U). See also corresponding Movie S7 and Movie S8.

conventionally used materials (nanoparticles or liquid metals). As a result, such particle structures could be used for various electronic applications. In the following example, we show how to deposit particles on a substrate to form conductive micropaths.

First, we produced a long particle chain composed of hundreds of solder balls (~200 μm) initially dispersed in a liquid flux. Then, the particles were deposited on a glass substrate by simultaneously translating the substrate and lowering the electrode to which the particle chain was attached (see Fig. 8a). The final shape of the deposited particle structure is governed by the motion of the substrate. As presented in Fig. 8a, a simple linear pattern was made in around 10 s.

The as-deposited micropath was poorly conductive owing to the small contact area between particles. Therefore, a postprocessing step is required to improve the electrical conductance. The conductance can be increased through heat or pressure sintering leading to the formation of a solid mass of material or by other means. Here, we demonstrate that mechanical compression can be used to increase the contact area, and thus the conductance of the particle chain. In Fig. 8b, we show three images (taken from above in direction along the compressive force) of 250-μm solder particles compressed by 6 %, 21 %, and 45 %. The particle chain was deposited on a carrier with two gold pads designed for impedance measurements (see Fig. S4) so that we could simultaneously measure the resistance of the chain and study the shape of the compressed particles. In Fig. 8c, we present COMSOL results of the simulated shape changes of the compressed solder balls, with the blue area denoting the contact area between neighboring balls. In Fig. 8d, we plot (dashed curve) the theoretically estimated (based on COMSOL results) values of resistance of 250-μm solder balls forming a conductive path between 1.6-mm distanced electrical contacts and compare them with the experimental results (red circles). The results show that the theoretical and experimental data match qualitatively although the experimental values are consistently smaller. With our ongoing research project, we hope to find out the reason for this discrepancy. Nevertheless, it is interesting to note that even a small deformation of a few % leads to a reduction in resistance by several order of magnitudes. Eventually, with a further compression, the resistance becomes very low, reaching a range of mΩ.

4. Discussion and conclusions

Within this work, we developed and explored the electric method for efficient formation of 1D particle structures. We studied in detail the influence of different parameters (such as electric field tension, size and shape of particles, viscosity, and ionic conductivity of the medium liquid) on the assembly process and the stability of the final particle chain.

Particles: Our results reveal that different types of microparticles (solid, core–shell, and soft particles) of any density can be assembled within seconds to form long chains. The particles should preferably be highly conductive to make a long chain, otherwise the voltage drop along the particle chain results in fast weakening of the electric force along the particle structure. Although, it was possible to form 1D structures using disc- or rod-shaped particles, the preferred shape is spherical. This is because the electric and capillary interactions between particles are much stronger for spherical particles. The spherical particles studied here had radii in the range of 20–500 μm. We failed to form long particle chains using particles larger than 500 μm. This is due to the increased significance of the gravitational force (see Table 1). In regard to the smallest particle size, in principle, it should be possible to go down

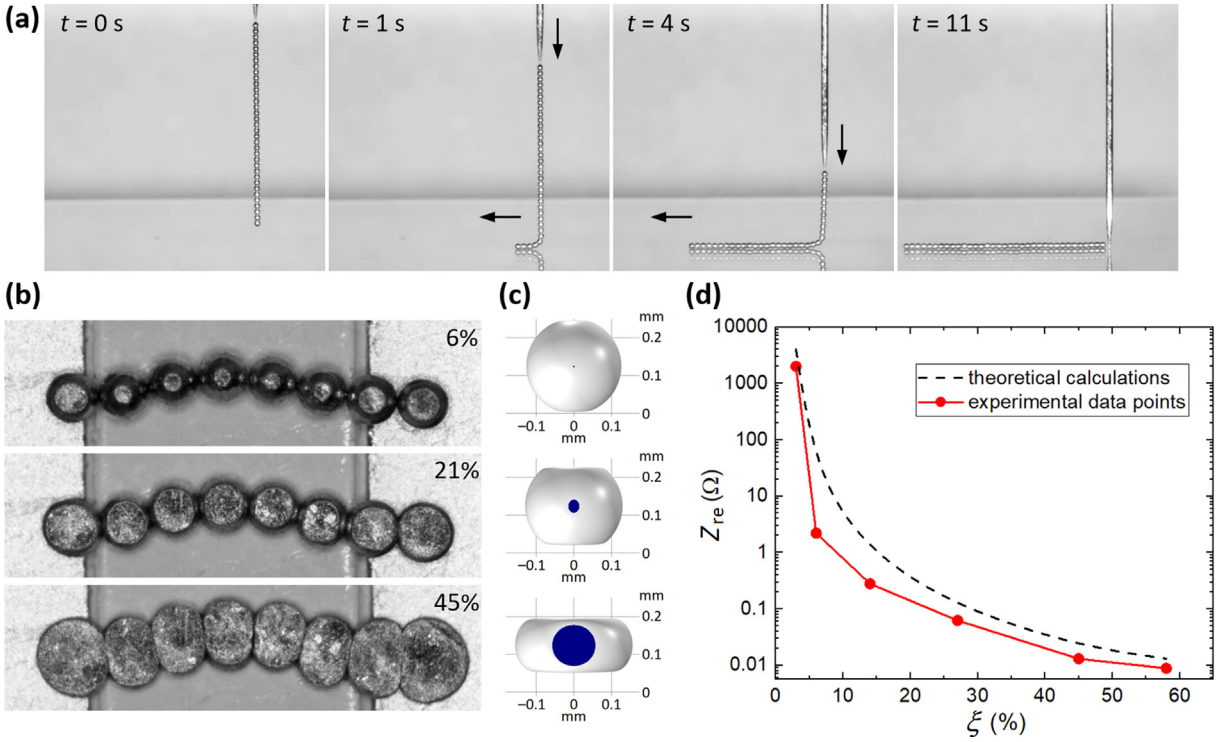

Fig. 8. (a) Solder particle chain (length of 0.74 mm) formed in air is deposited on a glass substrate by simultaneously translating the substrate and lowering the electrode. (b) Solder particles (size of 250-μm) deposited on a holder with two gold pads for impedance measurements. The chain was compressed by 6 %, 21 % and 45 % in direction along the viewing direction. (c) COMSOL simulated shapes of compressed solder balls with blue area denoting the contact area between neighboring balls. The degrees of the compression correspond to those from the experiment shown in panel b. (d) Experimental data and theoretically estimated values of the resistance (Z_{re}) plotted against the degree of compression (ξ). (For interpretation of the references to colour in this figure legend, the reader is referred to the web version of this article.)

below 1 μm. We attempted to form chains using spherical particles with radii of around 8 μm. However, the success rate was low and only short (several particle long) chains could be formed. Those small particles agglomerated more readily than larger particles of the same material, preventing successful formation of 1D structures outside liquid. Thin 1D particle structures (below 20 μm) are fragile and more prone to breaking. Therefore, stable experimental conditions are required, *i.e.*, eliminating micro vibrations of the experimental setup, wind draft in the lab, etc. It is worth mentioning that unlike in the methods described in ref. [54–58], the particles need no special pretreatment (functionalization) to form a stable 1D structure after the process of their formation is finished. The stability of the structure is attributed to the attractive interactions of capillary liquid bridges formed between neighboring particles.

Liquids: We showed that different types of dispersing liquids can be used. This ability to combine different particles with different liquids has practical relevance. For example, the liquid flux coats solder particles preventing the formation of an undesired passivation layer on the particle's surface and may promote particle sintering (if the 1D solder particle structure is to be used, for example, for electronic applications). On the other hand, the UV-hardened epoxy or paraffin wax may influence the particle chain flexibility. It can be also used to permanently lock particles (see Fig. S5) and form 1D, out-of-plane structures to be used, for example, as simple artificial cilia or cantilever arrays for robotics or sensors. Our experimental results reveal that liquids with large viscosity and low ionic conductivity are preferred as they reduce the negative effect of ionic screening, affecting the strength and frequency of the applied electric tension.

1D structure: We found that capillary forces help aligning particles and create one particle–thick structures preventing agglomerate formation. Additionally, we estimated the optimal pulling conditions to form a 1D particle structure that remains stable after turning off the electric tension. The maximum pulling velocity is primarily determined by the particle size and liquid viscosity. Interestingly, as shown in Fig. 3d, a binary microstructure can be formed using a dispersion of two types of particles having different size. Such structures may be desired, for example, for creating particle-based superstructures [59]. We also took advantage of the possibility of creating freestanding 1D structures to investigate their mechanical properties. The results indicate that the mechanical properties, including the stiffness of the primary 1D structure, are greatly affected by the strength of electric tension in a nontrivial fashion. This has not been studied before. Therefore, we are now running a follow-up project to understand in detail the influence of electric potential on the mechanics of one particle–thick assemblies aiming to generate new knowledge in this research area. Another thing to note is that high electric tensions may lead to formation of agglomerated rather than one particle–thick structures (see ref. [50]).

Example of applications: We also investigated possibilities of future application of beaded chains, including formation of conductive pathways on substrates for use in a variety of electronic applications. We are aware that the scheme presented in Fig. 8a–c may be impractical, especially in the industry settings. Still, the experimental results show the feasibility of the concept of using electric and capillary interactions for creating one particle–thick micropaths. This, in turn, stimulated us to explore the possibility of simultaneous formation of particle chains and their alignment on a substrate, which will ultimately enable the deposition of thousands of microparticles per second in a continuous manner [60]. We, therefore, foresee the method (which relies on the interplay between electric force, gravitational force, and the force stemming from capillary interactions) to be potentially useful in the display sector (open defect repair technology, fabrication of transparent conductive films), smart glass industry, security printing, and more.

Author contributions

Z. Rozynek initiated the project, formulated the scientific hypotheses, co-designed all experiments, and performed the experiments with results presented in Figs. 3a,d,e,h, Figs. 4a,c, Fig. 5, Fig. 6, Figs. 7a–e,g, Fig. S1a, Fig. S1b, Fig. S2, Fig. S3 and Fig. S5. Y. Harkavyi co-designed and performed experiments with results shown in Fig. 2, Fig. 3b,c,f,g, Fig. 4b, Fig. 8a,b, Fig. S1c, and Fig. S4. K. Giżyński co-designed and performed the experiments with results presented in Fig. 8c,d. Z. Rozynek wrote the first version of the manuscript. All authors took part in discussions toward the finalization of the manuscript. Z. Rozynek administered the submission and the review process.

Data availability

No data was used for the research described in the article.

Declaration of Competing Interest

The authors declare that they have no known competing financial interests or personal relationships that could have appeared to influence the work reported in this paper.

Acknowledgements

This research was funded by the Polish National Science Centre through OPUS (Grant No. 2019/33/B/ST5/00935) and SONATA (Grant No. 2019/35/D/ST5/03613) programs. We wish to thank Dr. A. Magdziarz, the owner of the company CADENAS in Poland, for giving us access to the company's research infrastructure and for providing materials. We also thank K. Kacprzak who performed some of the preliminary experiments that led to creation of Fig. 6, T. Kubiak who performed some of the preliminary experiments that led to creation of Fig. 7f, and Dr. F. Dutka for his help in calculating the capillary interactions (results presented in Fig. 4a and Fig. 5b).

Appendix A. Supplementary material

Supplementary data to this article can be found online at https://doi.org/10.1016/j.matdes.2022.111233.

References

[1] O.D. Velev, S. Gupta, Materials Fabricated by Micro- and Nanoparticle Assembly – The Challenging Path from Science to Engineering, Adv. Mater. 21 (19) (2009) 1897–1905.
[2] K.W. Allen, A. Darafsheh, F. Abolmaali, N. Mojaverian, N.I. Limberopoulos, A. Lupu, V.N. Astratov, Microsphere-chain waveguides: Focusing and transport properties, Appl. Phys. Lett. 105 (2) (2014) 021112.
[3] T. Mitsui, T. Onodera, Y. Wakayama, T. Hayashi, N. Ikeda, Y. Sugimoto, T. Takamasu, H. Oikawa, Influence of micro-joints formed between spheres in coupled-resonator optical waveguide, Opt. Express 19 (22) (2011) 22258–22267.
[4] W. Ahn, X. Zhao, Y. Hong, B.M. Reinhard, Low-Power Light Guiding and Localization in Optoplasmonic Chains Obtained by Directed Self-Assembly, Sci. Rep. 6 (1) (2016).
[5] M. Gao, M. Kuang, L. Li, M. Liu, L. Wang, Y. Song, Printing 1D Assembly Array of Single Particle Resolution for Magnetosensing, Small 14 (19) (2018) 1800117.
[6] K. Xu, L. Qin, J.R. Heath, The crossover from two dimensions to one dimension in granular electronic materials, Nat. Nanotechnol. 4 (6) (2009) 368–372.
[7] T. Ludtke, P. Mirovsky, R. Huther, L. Gover, G.H. Bauer, J. Parisi, R.J. Haug, Transport in nanoparticle chains influenced by reordering, Phys. Lett. A 375 (20) (2011) 2079–2081.
[8] M. Su, F. Li, S. Chen, Z. Huang, M. Qin, W. Li, X. Zhang, Y. Song, Nanoparticle Based Curve Arrays for Multirecognition Flexible Electronics, Adv. Matter. 28 (7) (2016) 1369–1374.
[9] A. Hubler, C. Stephenson, D. Lyon, R. Swindeman, Fabrication and Programming of Large Physically Evolving Networks, Complexity 16 (5) (2011) 7–8.

[10] X.Y. Jiang, J.G. Feng, L. Huang, Y.C. Wu, B. Su, W.S. Yang, L.Q. Mai, L. Jiang, Bioinspired 1D Superparamagnetic Magnetite Arrays with Magnetic Field Perception, Adv. Matter. 28 (32) (2016) 6952–6958.
[11] A. Spatafora-Salazar, L.H.P. Cunha, S.L. Biswal, Periodic deformation of semiflexible colloidal chains in eccentric time-varying magnetic fields, J. Phys.: Condensed Matter. 34 (18) (2022) 184005.
[12] D. Nishiguchi, J. Iwasawa, H.R. Jiang, M. Sano, Flagellar dynamics of chains of active Janus particles fueled by an AC electric field, New J. Phys. 20 (2018) 015002.
[13] S. Gangwal, A. Pawar, I. Kretzschmar, O.D. Velev, Programmed assembly of metallodielectric patchy particles in external AC electric fields, Soft Matter 6 (7) (2010) 1413–1418.
[14] S. Gupta, R.G. Alargova, P.K. Kilpatrick, O.D. Velev, On-chip electric field driven assembly of biocomposites from live cells and functionalized particles, Soft Matter 4 (4) (2008) 726–730.
[15] B. Bharti, G.H. Findenegg, O.D. Velev, Co-Assembly of Oppositely Charged Particles into Linear Clusters and Chains of Controllable Length, Sci. Rep. 2 (1004) (2012) 1–5.
[16] H.R. Vutukuri, A.F. Demirors, B. Peng, P.D.J. van Oostrum, A. Imhof, A. van Blaaderen, Colloidal Analogues of Charged and Uncharged Polymer Chains with Tunable Stiffness, Angew. Chem. Int. 51 (45) (2012) 11249–11253.
[17] Z. Wang, Z. Wang, J. Li, Y. Wang, Directional and Reconfigurable Assembly of Metallodielectric Patchy Particles, ACS Nano 15 (3) (2021) 5439–5448.
[18] D. Guo, C. Li, Y. Wang, Y.N. Li, Y.L. Song, Precise Assembly of Particles for Zigzag or Linear Patterns, Angew. Chem. Int. 56 (48) (2017) 15348–15352.
[19] T. Mitsui, Y. Wakayama, T. Onodera, Y. Takaya, H. Oikawa, Observation of light propagation across a 90 degrees corner in chains of microspheres on a patterned substrate, Opt. Lett. 33 (11) (2008) 1189–1191.
[20] Y.D. Yin, Y. Lu, B. Gates, Y.N. Xia, Template-assisted self-assembly: A practical route to complex aggregates of monodispersed colloids with well-defined sizes, shapes, and structures, JACS 123 (36) (2001) 8718–8729.
[21] K. Brassat, F. Assion, U. Hilleringmann, J.K.N. Lindner, Self-organization of nanospheres in trenches on silicon surfaces, Phys. Status Solidi A 210 (8) (2013) 1485–1489.
[22] O. Lecarme, T.P. Rivera, L. Arbez, T. Honegger, K. Berton, D. Peyrade, Colloidal optical waveguides with integrated local light sources built by capillary force assembly, J. Vacuum Sci. Tech. B 28 (6) (2010) C6011–C6015.
[23] Y. Hong, W. Ahn, S.V. Boriskina, X. Zhao, B.M. Reinhard, Directed Assembly of Optoplasmonic Hybrid Materials with Tunable Photonic-Plasmonic Properties, J. Phys. Chem. Lett. 6 (11) (2015) 2056–2064.
[24] S.R. Chen, M. Su, C. Zhang, M. Gao, B. Bao, Q. Yang, B. Su, Y.L. Song, Fabrication of Nanoscale Circuits on Inkjet-Printing Patterned Substrates, Adv. Mater. 27 (26) (2015) 3928–3933.
[25] S. Vyawahare, K.M. Craig, A. Scherer, Patterning lines by capillary flows, Nano Lett. 6 (2) (2006) 271–276.
[26] K.Y. Suh, Surface-tension-driven patterning: Combining tailored physical self-organization with microfabrication methods, Small 2 (7) (2006) 832–834.
[27] T. Mitsui, Y. Wakayama, T. Onodera, Y. Takaya, H. Oikawa, Light propagation within colloidal crystal wire fabricated by a dewetting process, Nano Lett. 8 (3) (2008) 853–858.
[28] A.R. Tao, J. Huang, P. Yang, Langmuir−Blodgettry of Nanocrystals and Nanowires, Acc. Chem. Res. 41 (12) (2008) 1662–1673.
[29] R.R. Collino, T.R. Ray, R.C. Fleming, C.H. Sasaki, H. Haj-Hariri, M.R. Begley, Acoustic field controlled patterning and assembly of anisotropic particles, Extreme Mech. Lett. 5 (2015) 37–46.
[30] X.Y. Ling, I.Y. Phang, H. Schönherr, D.N. Reinhoudt, G.J. Vancso, J. Huskens, Freestanding 3D supramolecular particle bridges: fabrication and mechanical behavior, Small 5 (12) (2009) 1428–1435.
[31] T. Kraus, L. Malaquin, E. Delamarche, H. Schmid, N.D. Spencer, H. Wolf, Closing the gap between self-assembly and microsystems using self-assembly, transfer, and integration of particles, Adv. Mater. 17 (20) (2005) 2438–2442.
[32] C. Ladd, J.H. So, J. Muth, M.D. Dickey, 3D Printing of Free Standing Liquid Metal Microstructures, Adv. Mater. 25 (36) (2013) 5081–5085.
[33] F. Garcia-Santamaria, H.T. Miyazaki, A. Urquia, M. Ibisate, M. Belmonte, N. Shinya, F. Meseguer, C. Lopez, Nanorobotic manipulation of microspheres for on-chip diamond architectures, Adv. Matter. 14 (16) (2002) 1144–1147.
[34] S. Zimmermann, T. Tiemerding, S. Fatikow, Automated Robotic Manipulation of Individual Colloidal Particles Using Vision-Based Control, IEEE ASME Trans. Mechatron. 20 (5) (2015) 2031–2038.
[35] S. Yang, V.N. Astratov, Spectroscopy of coherently coupled whispering-gallery modes in size-matched bispheres assembled on a substrate, Opt. Lett. 34 (13) (2009) 2057–2059.
[36] V.N. Astratov, J.P. Franchak, S.P. Ashili, Optical coupling and transport phenomena in chains of spherical dielectric microresonators with size disorder, Appl. Phys. Lett. 85 (23) (2004) 5508–5510.
[37] N. Kang, J. Zhu, et al., Reconfiguring Self-Assembly of Photoresponsive Hybrid Colloids, J. Am. Chem. Soc. 144 (11) (2022) 4754–4758.
[38] Z. Rozynek, M. Han, F. Dutka, P. Garstecki, A. Józefczak, E. Luijten, Formation of printable granular and colloidal chains through capillary effects and dielectrophoresis, Nat. Commun. 8 (2017) 15255.
[39] W.H. Yeo, J.H. Chung, Y.L. Liu, K.H. Lee, Direct concentration of circulating DNA by using a nanostructured tip, in: M. Razeghi, H. Mohseni (Eds.), Biosensing, 7035, SPIE, 2008, p. 70350N.
[40] J. Tang, B. Gao, H.Z. Geng, O.D. Velev, L.C. Qin, O. Zhou, Assembly of 1D nanostructures into sub-micrometer diameter fibrils with controlled and variable length by dielectrophoresis, Adv. Mater. 15 (16) (2003) 1352–1355.
[41] J. Ma, J. Tang, Q. Cheng, H. Zhang, N. Shinya, L.C. Qin, Effects of surfactants on spinning carbon nanotube fibers by an electrophoretic method, Sci. Technol. Adv. Mater. 11 (6) (2010) 1–7.
[42] J.H. Han, G.L.C. Paulus, R. Maruyama, D.A. Heller, W.J. Kim, P.W. Barone, C.Y. Lee, J.H. Choi, M.H. Ham, C. Song, C. Fantini, M.S. Strano, Exciton antennas and concentrators from core-shell and corrugated carbon nanotube filaments of homogeneous composition, Nat. Mater. 9 (10) (2010) 833–839.
[43] R. Maruyama, Y.W. Nam, J.H. Han, M.S. Strano, Well-defined single-walled carbon nanotube fibers as quantum wires: Ballistic conduction over micrometer-length scales, Curr. Appl. Phys. 11 (6) (2011) 1414–1418.
[44] J.H. Shin, K. Kim, T. An, W. Choi, G. Lim, Reliable Diameter Control of Carbon Nanotube Nanobundles Using Withdrawal Velocity, Nanoscale Res. Lett. 11 (2016) 1–6.
[45] S.J. Kahng, J.H. Kim, J.H. Chung, Nanostructured Tip-Shaped Biosensors: Application of Six Sigma Approach for Enhanced Manufacturing, Sensors 17 (1) (2017) 1–17.
[46] W.H. Yeo, F.L. Chou, K. Oh, K.H. Lee, J.H. Chung, Hybrid Nanofibril Assembly Using an Alternating Current Electric Field and Capillary Action, J. Nanosci. Nanotechnol. 9 (12) (2009) 7288–7292.
[47] B. Yuan, L. Cademartiri, Flexible One-Dimensional Nanostructures: A Review, J. Mater. Sci. Technol. 31 (6) (2015) 607–615.
[48] J.L. Breidenich, M.C. Wei, G.V. Clatterbaugh, J.J. Benkoski, P.Y. Keng, J. Pyun, Controlling length and areal density of artificial cilia through the dipolar assembly of ferromagnetic nanoparticles, Soft Matter 8 (19) (2012) 5334–5341.
[49] L.J. Hill, J. Pyun, Colloidal Polymers via Dipolar Assembly of Magnetic Nanoparticle Monomers, ACS Appl. Mater. Interfaces 6 (9) (2014) 6022–6032.
[50] A. Mikkelsen, A. Kertmen, K. Khobaib, M. Rajňák, J. Kurimský, Z. Rozynek, Assembly of 1D Granular Structures from Sulfonated Polystyrene Microparticles, Materials 10 (10) (2017) 1212.
[51] F. Dutka, Z. Rozynek, M. Napiórkowski, Continuous and discontinuous transitions between two types of capillary bridges on a beaded chain pulled out from a liquid, Soft Matter 13 (27) (2017) 4698–4708.
[52] I. Sriram, R. Walder, D.K. Schwartz, Stokes-Einstein and desorption-mediated diffusion of protein molecules at the oil–water interface, Soft Matter 8 (22) (2012) 6000–6003.
[53] B. Bharti, A.L. Fameau, M. Rubinstein, O.D. Velev, Nanocapillarity-mediated magnetic assembly of nanoparticles into ultraflexible filaments and reconfigurable networks, Nat. Mater. 14 (11) (2015) 1104.
[54] D.C. Li, J. Rogers, S.L. Biswal, Probing the Stability of Magnetically Assembled DNA-Linked Colloidal Chains, Langmuir 25 (16) (2009) 8944–8950.
[55] V.T. Mukundan, M.N.T. Quang, Y.H. Miao, A.T. Phan, Connecting magnetic micro-particles with DNA G-quadruplexes, Soft Matter 9 (1) (2013) 216–223.
[56] A. Demortiere, A. Snezhko, M.V. Sapozhnikov, N. Becker, T. Proslier, I.S. Aranson, Self-assembled tunable networks of sticky colloidal particles, Nat. Commun. 5 (2014) 3117.
[57] M. Motornov, S.Z. Malynych, D.S. Pippalla, B. Zdyrko, H. Royter, Y. Roiter, M. Kahabka, A. Tokarev, I. Tokarev, E. Zhulina, K.G. Kornev, I. Luzinov, S. Minko, Field-Directed Self-Assembly with Locking Nanoparticles, Nano Letters 12 (7) (2012) 3814–3820.
[58] J. Byrom, P. Han, M. Savory, S.L. Biswal, Directing Assembly of DNA-Coated Colloids with Magnetic Fields To Generate Rigid, Semiflexible, and Flexible Chains, Langmuir 30 (30) (2014) 9045–9052.
[59] D. Guo, Y.N. Li, X. Zheng, F.Y. Li, S.R. Chen, M.Z. Li, Q. Yang, H.Z. Li, Y.L. Song, Programmed Coassembly of One-Dimensional Binary Superstructures by Liquid Soft Confinement, JACS 140 (1) (2018) 18–21.
[60] Z. Rozynek, V.N. Manoharan, et al. Efficient formation of one particle–thick microstructures on a substrate by direct writing (in preparation 2022).